THE ASTROPHYSICAL JOURNAL, 390:622–633, 1992 May 10

LIMITS ON THE MAGNETIC FLUX OF PRE–MAIN-SEQUENCE STARS

GIBOR BASRI,[1] GEOFFREY W. MARCY,[2] AND JEFF A. VALENTI[1]
Astronomy Department, University of California, Berkeley
Received 1991 April 3; accepted 1991 November 12

ABSTRACT

We attempt to detect magnetic fields on two weak–emission-line T Tauri stars by searching for the enhancement of the *equivalent widths* of Zeeman-sensitive absorption lines. For both stars, we synthesize 26 observed Fe I lines, which represent a wide range of Zeeman sensitivities, using an LTE Stokes line-transfer calculation. The theoretical growth of equivalent width with magnetic field is discussed for lines with various Zeeman patterns. Oscillator strengths for all lines are empirically determined a priori using a magnetically quiet star of similar spectral type. The iron abundances of both T Tauri stars are established by synthesizing lines that are insensitive to Zeeman splitting.

We find that the observed equivalent widths of Zeeman-sensitive lines in TAP 35 are systematically enhanced relative to those calculated for no magnetic field, while such an enhancement is not seen in Zeeman-insensitive lines. The excess W_{eq} of Zeeman lines can be explained by a field of ~ 1000 G covering the entire surface, or by stronger fields covering proportionately less of the surface. With greater certainty, an upper limit can be placed on the product: $Bf < 1500$ G for TAP 35. If fields do cover a significant fraction of the surface, the strength is likely less than 3000 G, based on the lack of Zeeman broadening in the most Zeeman sensitive lines. Our method is not sensitive to the presence of fields in dark starspots. No Zeeman enhancement of line equivalent widths is seen in TAP 10, which provides an upper limit to its magnetic flux of $Bf < 700$ G. This magnetic nondetection is consistent with the apparently weaker chromospheric activity on that star as measured by the Ca II infrared triplet emission.

Subject headings: stars: magnetic fields — stars: pre–main-sequence

1. INTRODUCTION

Many characteristics of pre–main-sequence stars suggest the presence of surface magnetic fields. Spectroscopically, T Tauri stars (TTS) exhibit a wide variety of emission lines such as Hα, Ca II H and K, and Fe II at optical wavelengths, as well as lines of Mg II, Si I, C IV, S IV, and He II in the UV, all reminiscent of the spectrum of active magnetic regions on the Sun (see Herbig 1970; Imhoff & Giampapa 1982). These lines must form above the photosphere in gas at 10^4–10^5 K that is heated by some nonradiative heating process, perhaps related to magnetic fields. In the weak-emission T Tauri stars (WTTS) the emission lines are narrow (< 50 km s^{-1}) and deep chromosphere models are successful in reproducing the observed line fluxes and continua. Supporting this, the absorption spectra of moderate TTS, when divided by spectra of normal main-sequence stars, show filling-in ("veiling") by amounts explainable with a deep chromospheric source function (Finkenzeller & Basri 1987). Since WTTS show no signs of a wind or accretion disk, it is reasonable to suspect that the lines all arise from a magnetically heated chromosphere similar to active regions on the Sun. The WTTS UV line fluxes are typically 10–50 times solar levels, which suggests a corresponding enhancement in the magnetic fields on WTTS relative to the Sun, of which only $\sim 2\%$ of the surface is covered by kilogauss fields. Thus one might expect TTS to contain kilogauss magnetic fields covering a large fraction of their surfaces.

Another magnetic indicator for WTTS is their X-ray luminosity which is $\sim 10^3$ times solar, indicative of strong coronae (Walter 1987). Indeed, X-ray luminosity for TTS correlates well with rotation (Bouvier 1990), as expected if coronal heating depends (via MHD dissipation) on surface magnetic fields generated in a dynamo. Optical photometric variations in WTTS (typically ~ 0.2 mag) have been attributed to cool starspots with surface filling factors of 0.1–0.4 (e.g., Vrba et al. 1989). Finally, many WTTS show short time-scale flarelike variability in X-rays (Montmerle et al. 1983) and radio emission (Cohen & Bieging 1986) which, in the absence of significant boundary-layer emission from these weak-lined stars, indicates that the emission source is close to the surface, presumably in magnetic regions. Indeed, the short time-scale variability in X-rays from WTTS is thought to be inconsistent with thermal bremsstrahlung (Feigelson 1987) but rather requires some nonthermal injection of energy, perhaps magnetic.

The more active classical TTS may also contain a deep chromosphere, but its emission may be overwhelmed by that due to accretion and/or outflow. The solar analogy is inadequate for the formation of some of the CTTS emission lines since the widths and strengths of some, notably broad Hα, Ca II, and Mg II, cannot be reproduced theoretically in the context of a "deep chromosphere" (Cram 1979; Calvet, Basri, & Kuhi 1984), thus casting doubt on magnetic fields as the energy source for the heating. Doubt also arises owing to the lack of correlation between Hα emission and rotation in TTS as would be expected if a dynamo generates the magnetic fields (Hartmann et al. 1986). Clearly, lines of Hα, Ca II, and Mg II, when broad, ~ 500 km s^{-1}, originate in a more extended dense circumstellar region.

Magnetic fields on TTS have been invoked to explain many phenomena. In addition to those cited above as possible evidence of magnetic fields, they figure prominently in current explanations of the angular momentum and mass loss from

[1] Astronomy Department, University of California, Berkeley, CA 94720.
[2] On leave from San Francisco State University; postal address: Department of Physics & Astronomy, San Francisco State University, San Francisco, CA 94132.

young stars during their accretion phase. These include Alfvén wave winds (Lago 1984; Hartmann et al. 1990), centrifugal winds (Shu et al. 1988; Königl 1989), magnetic braking (Königl 1991) and boundary-layer variability (Bertout, Basri, & Bouvier 1988; Basri 1991). In most cases, kilogauss fields covering most of the star would be sufficient.

To date, however, magnetic fields have not been directly detected on TTS. Spectropolarimetric efforts to detect the Zeeman effect in lines have been unsuccessful, perhaps because the fields are locally bipolar thereby cancelling the net longitudinal field (Brown & Landstreet 1981; Johnstone & Penston 1986, 1987). Zeeman broadening of photospheric lines is difficult to detect because of the dominance of rotational broadening ($v \sin i \sim 20$ km s^{-1}), although this approach would work if a bright, pole-on TTS could be found.

We describe in this paper a Zeeman technique that makes use of the enhancement of the *equivalent widths* of absorption lines owing to the wavelength shifting of the polarized line-absorption components in the presence of a magnetic field. This is the first application of such a technique to solar-type stars, though variations of it have been used for stars with greater fields such as Ap stars and white dwarfs. The technique involves observing absorption lines of different Zeeman sensitivities in the WTTS TAP 35 and TAP 10, and in several comparison stars and then making careful stellar model atmospheric calculations to predict the behavior of the lines with and without magnetic fields. The organization of the paper is as follows. Section 2 contains a description of the observations and the measurement of equivalent widths. Section 3 describes the method of synthesizing the lines, including choice of atmospheric parameters and determination of oscillator strengths, as well as the effect of Zeeman broadening. Section 4 describes the Zeeman analysis applied to the TTS.

2. OBSERVATIONS

We obtained observations using the Lick Observatory coudé echelle spectrometer ("Hamilton") and 800^2 TI CCD which gives a resolution of 40,000 and has partial wavelength coverage from 5000 to 8600 Å. This setting covers several Zeeman-sensitive lines, notably, λ8468 and λ6173, as well as several lines having very low Landé g values. We chose to target two brighter weak TTS, TAP 35 (= NTTS 042417 +1744, K1, V = 11), and TAP 10(NE) (= NTTS 035120 +3154NE, G5, V = 12) identified by Walter et al. (1988). They were selected because of their weak Hα emission and lack of IR excess, which leaves their photospheric absorption lines relatively uncontaminated by emission from a stellar wind or circumstellar disk. These two stars have rotation velocities and X-ray luminosities near average for WTTS (Hartmann et al. 1986; Walter et al. 1988) and thus their magnetic properties are not expected to be biased relative to common TTS.

For TAP 35 we obtained four exposures, totaling 3.6 hr, on the 3 m telescope on 1988 December 2, yielding a final signal-to-noise ratio in the summed spectrum of $\sim$100 : 1; slightly higher in the near IR than in the yellow region. For TAP 10, we obtained three exposures on the same date with a total exposure of 5 hours, obtaining a signal-to-noise ratio of $\sim$75 in the summed spectrum. We obtained at other times similar spectra of several comparison stars of similar spectral type, namely, τ Ceti (G8V), 61 U Ma (G8V), ϵ Eri (K2V), and ξ Boo A (G8V). The data were reduced in a standard way: the raw CCD images were divided by normalized flat-field exposures of an incandescent lamp, corrected for scattered light by subtracting the signal between orders, mashed into 54 individual spectral orders, and wavelength-calibrated using exposures of a Th-Ar lamp. A representative sample of the spectra near the Zeeman-sensitive line λ8468, is shown in Figure 1.

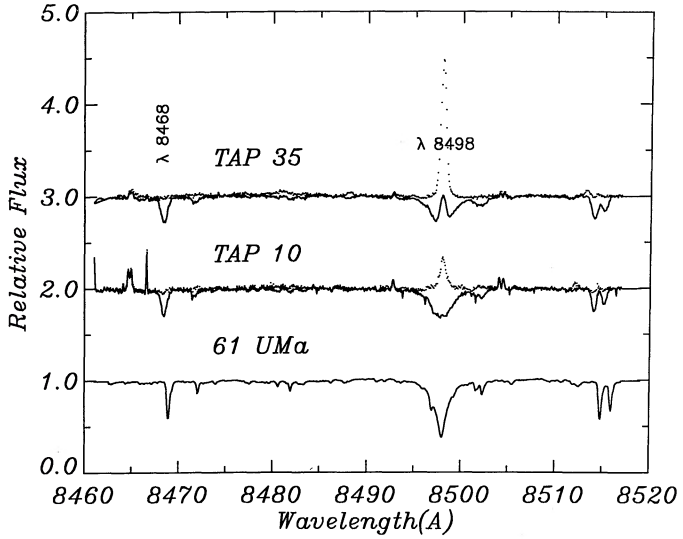

FIG. 1.—One spectral order each from (from top down): TAP 35, TAP 10, and 61 UMa. At the left the magnetically sensitive line λ8468 can be seen, and near the middle the activity-sensitive Ca II triplet line λ8468 shows filling in and emission in the young stars compared to the relatively inactive main-sequence star. The narrow emission features most prominent in TAP 10 are telluric. Notice the obvious rotational broadening in the young stars. The dotted lines for the young stars are the result of dividing the spectra by an appropriate spectral standard, which gives a true measure of the chromospheric enhancement present.

We searched the echelle format for Fe I absorption lines amenable to measurement of equivalent width, rejecting lines that were either too weak or blended. We used the lists of Solanki & Stenflo (1985), augmented by our own calculations of Landé g factors for clean lines. The spectral coverage of the echelle is incomplete, especially at longer wavelengths. We then selected and rejected lines by visual inspection of both TTS spectra to assess the effects of the considerable rotational broadening which promotes blends and supresses the pseudo-continuum. The final list of 26 lines is given in Table 1, which gives wavelength, excitation of the lower level, oscillator strength (gf), and Landé g value, and the number of Zeeman components. The Landé g factor given is the "effective" factor, a weighted sum of the splittings of the components that persist for a magnetic field aligned along the line of sight, computed with straight LS coupling. The last column, to be discussed below, gives the ratio of calculated equivalent widths at $B = 1000$ G and $B = 0$ G and represents a measure of the sensitivity of W_{eq} to magnetic fields.

We carefully measured the equivalent width of each line in all stars by the following procedure. For TAP 35, the continuum level was determined by eye on both the left and right sides of the line, and a straight line was drawn between the two, under which the area of the line was computed by numerical integration. The continuum placement for such a rotationally broadened spectrum is subject to errors of several percent because of pervasive weak lines. The resulting measurements of

TABLE 1

LINES USED IN ZEEMAN ANALYSIS

Wavelength (Å)	χ_{ex} (eV)	log(gf)	Landé g	Zeeman Components	W_{eq}(1 kG)/W_{eq}(0 G)
5322.04.....	2.31	−3.03	0.667	15	1.048
5434.52.....	1.0	−2.47	0.000	3	1.000
5506.78.....	1.00	−3.02	2.000	15	1.071
5576.09.....	3.47	−0.85	0.000	3	1.000
6065.48.....	2.64	−1.71	0.667	3	1.009
6173.34.....	2.25	−3.00	2.500	3	1.178
6180.22.....	2.7	−2.74	0.625	21	1.047
6254.26.....	2.30	−2.10	1.500	3	1.049
6265.13.....	2.20	−2.55	1.583	19	1.102
6270.24.....	2.89	−2.71	0.500	3	1.011
6380.75.....	4.23	−1.49	0.667	3	1.018
6677.99.....	2.72	−1.47	1.100	27	1.033
6703.57.....	2.79	−3.23	0.900	3	1.024
6704.48.....	4.27	−1.55	0.250	9	1.064
7491.68.....	4.28	−1.10	1.500	9	1.167
7507.30.....	4.29	−1.22	1.167	15	1.074
7568.93.....	4.26	−0.70	1.500	15	1.095
7583.80.....	3.05	−1.99	0.833	15	1.038
7586.04.....	4.29	−0.26	1.300	27	1.051
7780.59.....	4.45	−0.13	0.833	15	1.023
8387.77.....	2.20	−1.35	1.500	15	1.060
8468.40.....	2.25	−2.19	2.500	3	1.232
8611.81.....	2.88	−1.90	1.500	3	1.125
8621.61.....	2.94	−2.21	1.200	3	1.086
8757.19.....	2.88	−1.87	1.500	3	1.130
8764.00.....	4.63	−0.02	0.667	3	1.023

W_{eq} can be in error by as much as 10% and are systematically underestimated due to this effect. To achieve consistent continuum placement for a particular line in all stars, we preserved plots showing the continuum placements for TAP 35 so that identical placement could be employed for all other stars. We found that any "automatic" algorithm for continuum determination occasionally erred owing to the rotational broadening of TAP 35 and nonuniform density of neighboring lines. We are therefore more confident of the relative accuracy of line measurements within our sample, and less confident of their absolute accuracy.

Before carrying out the measurement of equivalent widths for the main-sequence stars, we convolved their spectra with the rotational broadening function (Gray 1976) to $v \sin i = 17$ km s^{-1} (see § 3.3) so that the continuum placement and weak blends affected the measurements in the same way as with TAP 35. No artificial broadening of the TAP 10 spectrum was necessary because of its intrinsic rotational broadening. The resulting broadened spectra of the main-sequence stars were remarkably similar to that of TAP 35, although the Fe lines were clearly weaker in τ Ceti, an old disk star. The final measured equivalent widths are given in Table 2.

3. THE ZEEMAN METHOD

The basic approach in this Zeeman analysis is to detect an enhancement of the equivalent widths of Zeeman-sensitive lines above the values expected if there were no magnetic field. Modeling and fitting lines of low Zeeman sensitivity provides a determination of stellar parameters, namely, iron abundance, and T_{eff}, from which the lines of high Zeeman sensitivity can then be computed. Modeling these Zeeman-sensitive lines yields an estimate of the product of magnetic field strength, B, and surface filling factor f. We have chosen to model the line transfer of all 26 lines self-consistently to predict their equivalent widths as a function of the surface magnetic field.

The line-transfer technique has been described previously in detail (Basri & Marcy 1988). Briefly, we calculate in LTE the line transfer in all Stokes parameters, thus treating the Zeeman-induced polarization across each line profile. We construct model atmospheres for all stars by scaling $T(\tau)$ of the HM solar atmosphere (Holweger & Müller 1974) using their respective effective temperatures (see below), and recomputing the densities and ionization equilibria to satisfy self-consistently hydrostatic equilibrium and the Saha equation (Gray 1976). We use this atmosphere because it reproduces observed solar line depths (Holweger 1967; Rutten & Kostik 1982) in an LTE context that is easy to apply. Moreover, Rutten & Kostik argue that the structure of the HM model compensates for NLTE overionization of neutral iron in the photosphere and that the photospheric source function is in fact thermal. The main improvement for this work was to reconfigure our code to compute many lines with a specified grid of model parameters during one run.

3.1. *Oscillator Strengths*

Preliminary choices for oscillator strengths were taken from Fuhr, Martin, & Wiese (1987), many of which are based on the Oxford work (e.g., Blackwell, Petford, & Simmons 1982). Unfortunately, use of these gf-values and the HM solar atmosphere (in LTE) leads to discrepancies between calculated and observed (Kurucz et al. 1984) equivalent widths of several percent. The disagreement is correlated with line strength and

TABLE 2

OBSERVED EQUIVALENT WIDTHS (Å)

Wavelength	τ Ceti	61 UMa	ξ Boo A	ϵ Eri	TAP 10	TAP 35
5322.04	0.057	0.052	...	0.078	0.075	0.083
5434.52	0.219	...	...	...	0.204	0.222
5506.78	0.147	0.179	0.178	0.260	0.178	0.228
5576.09	0.131	0.166	0.161	0.205	0.149	0.164
6065.48	0.127	0.153	0.148	0.197	0.139	0.170
6173.34	0.065	0.083	0.082	0.099	0.087	0.113
6180.22	0.051	0.076	0.071	0.089	0.075	0.096
6254.26	0.122	0.165	0.152	0.169	0.159	0.186
6265.13	0.093	0.115	0.110	0.141	0.110	0.149
6270.24	0.046	...	...	0.078	0.060	0.073
6380.75	0.039	0.062	0.056	0.067	0.062	0.076
6677.99	0.146	0.178	0.175	0.246	0.173	0.196
6703.57	0.029	0.050	0.046	0.061	0.045	0.061
6704.48	0.035	0.061	0.056	0.066	0.055	0.068
7491.68	0.061	0.090	0.083	0.102	0.083	0.112
7507.30	0.053	0.085	0.072	0.102	0.073	0.084
7568.93	0.091	0.101	0.096	0.134	0.108	0.137
7583.80	0.083	0.101	0.094	0.122	0.099	0.121
7586.04	0.129	0.165	0.151	0.199	0.167	0.189
7780.59	0.129	0.170	0.159	0.204	0.152	0.174
8387.77	0.264	0.319	0.276	0.386	0.242	0.288
8468.40	0.137	0.167	0.169	0.220	0.208	0.224
8611.81	0.108	0.127	0.124	0.150	0.125	0.163
8621.61	0.082	0.091	0.085	0.119	0.095	0.113
8757.19	0.112	0.135	0.125	0.172	...	0.178
8764.00	0.130	0.175	0.167	0.219	0.143	0.149

excitation potential, such that the model equivalent widths grow too quickly. Use of these *gf*-values with a solar atmosphere scaled to another effective temperature (we tried 61 UMa and τ Ceti) leads to even larger discrepancies. We conclude that *the HM model is inconsistent with laboratory gf-values.* This is understandable, since the HM atmosphere was derived without using any laboratory *gf*-values. Its *gf*-values were chosen to produce the right equivalent widths, then the model was found by line depth matching. Furthermore the process of scaling the solar atmosphere to other effective temperatures is imperfect, as there is no guarantee that they actually have the same atmospheric structure.

In principle, the proper remedy assuming that laboratory *gf*-values are correct is to construct a model stellar atmosphere which minimizes the differences between calculated and observed equivalent widths. We have elected not to do this now, because it is an enormous effort in its own right. Instead, we calculate empirical *gf*-values using the star 61 UMa, as described below. This star is ~4 times as active as the Sun, but can be considered inactive in the context of this paper, since our method is only sensitive to magnetic fluxes much higher than that. One advantage of this empirical approach is that errors in our modeling procedure are partially compensated for by the *gf*-values we choose. These include errors in the HM model and the assumption of LTE as translated to other stars, and systematic errors in our measured equivalent widths due to unresolved blends.

The iron abundance, Fe/H, of 61 UMa was determined by synthesizing, for a range of assumed values of Fe/H, only the 10 lines in Table 1 for which laboratory *gf*-values of quality "C" or higher existed (Fuhr et al. 1987). For each of these lines, we determined the value of Fe/H that yield agreement between calculated and observed equivalent widths in 61 UMa. We adopted the average of these values of Fe/H as the best estimate for 61 UMa, giving log (Fe/H) = −4.53. All line transfer calculations were done using the HM solar atmosphere scaled to $T_{\rm eff}$ = 5250 and log (*g*) = 4.65. We did not try to adjust the abundances in the calculation of gas pressures or continuum optical scales, as work by Arribas & Crivellari (1989) has shown this to be of minor importance.

We then determined *gf*-values for all lines (including those having lab determinations) by synthesizing each for a range of trial *gf*-values and determining that value which yielded agreement between calculated and observed equivalent width. These empirical *gf*-values are tied to the lab values because the adopted iron abundance of 61 UMa was determined using lab values only. The final empirical *gf*-values, given in Table 1, scatter relative to the lab values by 0.2 dex. For two of the lines, λλ5434, 6270, the equivalent widths in 61 UMa were not measured because they were Doppler-shifted off the CCD. For these two lines, we simply adopted the lab *gf*-values from Fuhr et al. (1987).

These empirical *gf*-values raise several issues. First, their discrepancies relative to lab values are due to inadequacies both in the scaled model atmosphere for 61 UMa and in the assumption of LTE (in addition to errors in the measured equivalent widths.) These *gf*-values should best be considered "effective" values, since they represent the appropriate values to employ when using our imperfect scaled atmospheres in LTE and are based on equivalent widths which include blends and are measured with a continuum placement influenced by rotational broadening. In this sense, they may be preferred over lab values in an analysis using atmospheres similar to our 61 UMa model and with data like ours. However, these effective *gf*-values might well be inadequate if one uses them with stars having very different broadening or $T_{\rm eff}$. All six stars in

this study, including the WTTS, have adopted $T_{\rm eff}$ between 4900 and 5500 K, straddling that adopted for 61 UMa (G8V): 5250 K.

We tested the integrity of the effective *gf*-values by attempting to synthesize lines in ξ Boo A (G8V), τ Ceti (G8V, but low metallicity), and in ϵ Eri (K2V). For ξ Boo A, the observed and calculated equivalent widths of magnetically insensitive lines agreed to within 5% rms. The derived iron abundance was log (Fe/H) = −4.55. For ϵ Eri, there was 8% scatter, with log (Fe/H) = −4.41. The abundances derived here differ from those in Paper II, since there we used a single line to get them: λ7748. We also checked the effect of lowering the gravity for ϵ Eri to log (g) = 4.0 from 4.65. This increased the scatter to 10%. It appears that for atmospheric models somewhat different than that used to derive the *gf*-values, the ability of these *gf*-values to predict equivalent widths is compromised, with errors of up to 10%.

We also attempted to derive *gf*-values using τ Ceti, adopting atmospheric parameters for it from the fine analysis by Arribas & Crivellari (1989). Using their value of iron abundance and the lab *gf*-values, the calculated equivalent widths come out systematically too low by ~20%. A similar effect in the same direction was found by Arribas & Crivellari (1989) when they used the HM solar model. We derived a new iron abundance for τ Ceti which, when using lab *gf*-values and scaled HM atmosphere, yielded calculated equivalent widths that agreed on average with those observed. The final Fe abundace for τ Ceti was log (Fe/H) = −4.81 [compared with the solar value log (Fe/H) = −4.5]. The *gf*-values derived here from τ Ceti were not as effective in reproducing the equivalent widths for ξ Boo A as those derived from 61 UMa, with an rms scatter of 8%. Therefore, we used only the latter *gf*-values.

3.2. *Stellar Parameters*

One of the difficulties in studying line formation in TTS is that the stellar parameters needed to do a model atmospheric analysis are themselves poorly known, as well as the structure of the atmosphere itself. Spectral types of the WTTS were given by Walter et al. (1988), based on their colors and the appearance of the low dispersion spectrum. Although this is not likely to be a very precise procedure, we have no reason to doubt its basic accuracy. At the time we made the observations, we also observed two subgiants with the same spectral classes as given for the WTTS, hoping to use them as null stars and to check the spectral typing. As discussed by Basri & Batalha (1990), it turns out that subgiants are not good standards for TTS. We see the same problems here: the line strengths were all clearly too large in the subgiants compared to the TTS, and attempts to check the spectral types with temperature-sensitive line ratios were inconclusive. It is clear that main-sequence stars would have been better, and we are now accumulating a good set of standards to use at high resolution.

We decided instead to check that we had more or less the right atmosphere by studying the behavior of magnetically insensitive lines of varying excitation potentials as a function of effective temperature. Our test was simply to study the difference between observed and calculated equivalent widths versus excitation potential. One expects a slope (low excitation lines weak compared to high, or vice versa) when the atmosphere is too hot (or cold), and no slope when the temperature is correct. This check was made after determining the abundance at each temperature which gave the lowest overall scatter between observed and calculated equivalent widths for Zeeman insensitive lines regardless of excitation potential. We saw the expected behavior with effective temperature and were able to select temperatures with an internal error of 200 K or so. This test yielded a temperature of 5200 K for TAP 35. That is somewhat higher than the 4900–5000 K predicted by the spectral type of K1. The same test for TAP 10 yielded 5300 K which is a little low compared to its spectral type. We conclude that in order to obtain a precise spectral type from high dispersion line measurements, a good deal more work and a different (more temperature sensitive) set of lines will be required. We therefore tested our magnetic analyses with temperatures covering the plausible range for each star.

We actually ran a grid of both abundance and temperature for all our lines. This allowed us to select the best abundance after finally fixing temperature. Again we restricted ourselves to the insensitive lines, and we demanded that the average discrepancy between computed and observed equivalent widths be minimized. This led to log (Fe/H) = −4.21 for TAP 35 and −4.45 for TAP 10. All these calculations were done with the gravity arbitrarily set at log (g) = 4.0. Gravity is much more poorly known than effective temperature for TTS, as both the evolutionary tracks and observational determinations of stellar parameters are subject to uncertainty due to the possible past or current effects of disk accretion (e.g., Hartmann & Kenyon 1990), although this problem is less severe for the WTTS. The gravity should be lower than solar since the radii are likely to be larger and masses smaller for typical TTS, but it is also clear that it is probably not as low as in classical subgiants (because of the spectral discrepancies). We elected not to make gravity a real parameter, but instead checked at the end that our magnetic detection was not an artifact of choosing the wrong gravity.

The only stellar parameter that was easily and accurately determined is the projected rotation velocity. We selected a few clean nonmagnetic lines and spun up a standard star (making sure the lines had the same strength in it by scaling) until each profile was a very good fit to the observed WTTS profile. We were easily able to see which velocity worked best to within 1 km s^{-1}, since the rotation for these stars contributed more broadening than the spectrometer instrumental profile. The results were 17 km s^{-1} in TAP 35 and 12 km s^{-1} in TAP 10. These agree reasonably well with the results in Walter et al. (1988); ours are to be preferred since our data are of much higher quality.

3.3. *Magnetic Curve of Growth*

The transfer of line radiation in a magnetic field has recently been summarized by Jefferies, Lites, & Skumanich (1989). They redevelop in a complete and straightforward manner the transfer of the Stokes components of polarized radiation. In this work we only observe the intensity component, but it depends on the Q and V components as well (we have not included magneto-optic effects). We are searching for excess equivalent width in Zeeman sensitive lines over that seen in insensitive lines. Before we begin we must find a useful measure of magnetic sensitivity in this context. The effective Landé g factor is inadequate because we are not directly measuring the splitting of the components. The *equivalent width* of the final intensity profile of partially Zeeman-split lines is complicated by three issues. In increasing order of importance they are the polarization of the different Zeeman components, the extent to which individual components are "saturated" by themselves, and the total number and overlap of components (at a given magnetic

field strength). Regarding the first issue, we note that at any wavelength there may be a superposition of various Zeeman components, each capable of absorbing either linear or circularly polarized light. The extent to which they are present at a given wavelength depends on the Zeeman structure of the line, the magnetic field, and the line-of-sight angle.

The next important factor is the strength of individual components of a given polarization, once fully separated. To illustrate, consider two limiting cases. First, suppose we have a weak line on the linear portion of the curve of growth. The total equivalent width is independent of the extent to which the Zeeman components overlap, since even with zero field the individual opacities summed together do not saturate the line. Its equivalent width is therefore unaffected by magnetic fields, regardless of the line's effective Landé g factor! The Landé g factor does determine at what field strength Zeeman *broadening* of the line profile becomes detectable. At the other extreme, consider a strong line well into the flat portion of the curve of growth, in which many of the Zeeman components would be saturated even if by themselves. Now the total equivalent width of the line is extremely sensitive to the extent of overlap of the Zeeman components. When they overlap, the opacity provided by a single component has little additional effect on the total equivalent width. But when the components separate, each individual component adds nearly the equivalent width that was present in the null field (fully overlapped) case. In this extreme, the equivalent width of a strong fully separated line increases by a factor nearly equal to the number of components. In an intermediate case, the individual components end up much less deep than the null field line when separated, so the increase in equivalent width gained by separating the components (which makes the line cover a larger span of wavelength) is reduced by the effect of the components becoming shallower. This effect can be severe in some cases; it *is* severe for the lines chosen here in atmospheres below 4000 K. Which behavior is seen in a given case depends on a number of complicated factors and cannot be predicted solely on the basis of intrinsic line strength; the temperature gradient in the region of line formation is also quite important, for example.

The result is that equivalent width enhancement of a flux profile due to the Zeeman effect depends not only on the Landé g factor (which governs how much an individual component will shift at a given field strength) but also on the distribution and number of the π and σ Zeeman components over the profile. Note that quoted Landé g factors are usually weighted averages of the g factors for all the components, making it more difficult to assess how the line will grow based on that one number. As noted above, this growth also depends on the intrinsic strength of the line components, and furthermore will be different for different view angles. A detailed calculation is therefore required to fully predict the strength of the emergent flux profile.

There are three regimes of behavior for the equivalent width. In the case that the Zeeman splitting is small relative to the width of the Doppler core, an increment in field strength does little to increase W_{eq} because the Zeeman components are still mostly overlapping and only their outer edges move into the weak line wings. Thus dW_{eq}/dB is small. At larger field strengths, the splitting eventually becomes comparable to the core width (which depends somewhat on spectral type), at which point increases in field strength will result directly in a major incursion of components on both sides of the line into the formerly weak wings. In this regime, dW_{eq}/dB is as large as possible. Finally, when the Zeeman splitting becomes much greater than the Doppler core width the components are fully resolved from each other, at which point a further increase in B merely moves the components further apart from each other with no further increase in the total equivalent width. In this regime, dW_{eq}/dB becomes zero. Thus, the "magnetic curve of growth" looks more like the relation between exposure and density for photographic film than it does the classical curve of growth for spectral lines.

The field strength at which dW_{eq}/dB is greatest depends on the integrated "desaturation" of all of the Zeeman components that compose the line. Even lines with relatively low Landé g factors will, at some high field strength, achieve large values of dW_{eq}/dB (unless they are too weak). The above discussion implies that the amount of growth of a line depends more on the number of Zeeman components than on the effective Landé g value. Many atomic lines are composed of 10–20 Zeeman components thus permitting quite large increases in the equivalent width due to Zeeman broadening. *For field strengths greater than* $\sim$2 kG *in cool stars, the factor that typically dominates the growth in equivalent width is the number of Zeeman components, not the effective Landé g factor.* We have calculated the "magnetic curve of growth" for all of our lines in a G8V atmosphere, and six representative cases are shown in Figure 2. This figure shows the *fractional* increase of the equivalent width (over the zero field case) as a function of B. Each line has a "toe" at small field strengths, a regime of rapid growth with increasing field strength, and a plateau which occurs for large field strengths, as explained above. For most lines, this plateau occurs at larger field strengths than are shown, since they have Landé g factors less than 2.

The line exhibiting the largest growth at 5 kG is λ7491, which has doubled its equivalent width. (Note that we are referring to a field filling factor of unity.) It does so because of its modestly high Landé g factor, 1.5, and its relatively large number (9) of reasonably strong Zeeman components. The line λ8468 exhibits a rapid increase in equivalent width at rather small field strengths owing to its large Landé g factor (2.5) but ultimately does not grow as much as λ7491 because it has only three components. Note that λ6704, with a low Landé g factor of 0.25, nonetheless exhibits greater relative growth than λ8468

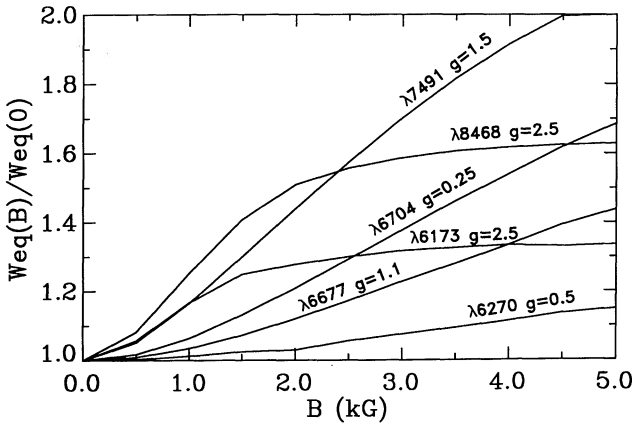

FIG. 2.—The "magnetic curve-of-growth" for representative lines in our sample. The Landé g factor for each line is indicated. The principles illustrated are explained in the text.

at 5 kG owing to its nine components. The line λ6173 grows less than λ8468 despite their identical Landé g factors because it is less saturated (weaker) and so the competing effects mentioned above limit its growth. The line λ6270, shown at bottom, grows very little owing to its small Landé g factor (0.5) and its few components (3). Finally, λ6677 is at first puzzling because it grows so little despite having a modest Landé g factor (1.1) and 27 (!) components. The reason for this odd behavior is that the 27 components are actually bunched rather closely together into three clumps, thus causing them to overlap and the line to remain saturated at 5 kG.

Because of these effects, a "magnetic sensitivity index" (S_B) for each line at a given field strength can be calculated by taking the calculated ratio of W_{eq} at that field to W_{eq} with no field, i.e., $S_{1000} = W_{eq}(1\,\mathrm{kG})/W_{eq}(0)$. This index depends (weakly) on the atmosphere under consideration, and we determine it using the TAP 35 atmosphere. Lines of highest sensitivity have S_{1000} of 1.15–1.20 (i.e., λλ6173, 7491, 8468), indicating that increases of 15%–20% will occur in kilogauss fields. This demonstrates the extent to which pervasive kilogauss fields are detectable by this technique and also indicates the accuracy which the measurements and modeling must achieve.

4. ZEEMAN ANALYSIS

4.1. *Magnetic Measurement*

Having measured a set of absorption lines and chosen their oscillator strengths, and having selected initial stellar parameters (as described in § 3), we are now in a position to try to determine the magnetic flux. The analysis by this point is actually quite simple. We run a grid of calculations for each line using the chosen temperature, abundance, and atmospheric structure in which we vary the magnetic field from zero to a chosen maximum value. For each field value, we obtain the equivalent width in each line. The ordinate of a diagnostic plot can then be computed as the ratio of an observed equivalent width to the calculated width with no magnetic field. It is directly comparable to the magnetic sensitivity index used as the abscissa, namely, S_B. One must choose a value of the field for the index, since the behavior of the equivalent widths of the lines depends on the field strength, line strength, and Zeeman structure of each line as described in the last section. We selected 1000 G after obtaining an initial estimate of what fields were apparently present. Thus, our index is $S_{1000} = W_{eq}(B = 1000)/W_{eq}(B = 0)$ as determined for each line by calculation; this is given in column (6) of Table 1.

For comparison we also show fits to the *calculated* ratios of W_{eq} at different field strengths to that for no field. With S_{1000} as abscissa, the zero field fit is a line with zero slope and unit intercept, and the 1000 G fit has unit slope and zero intercept. The shape of the curves at other field strengths depends on the details of the behaviors of the lines chosen, as discussed in § 3. The curves provided are actually quadratic fits to the results for the actual lines being used, which scatter somewhat about a smooth curve because of their individual behaviors.

The presence of a magnetic field is seen if the plotted points increase with S_{1000}, with a scatter not larger than that given by the low-sensitivity lines. Such lines have ratios which cluster near unity, of course, since their equivalent widths are not sensitive to the field. The observed ratios may differ from unity because of errors in the oscillator strength, measured equivalent width, and/or atmospheric parameters, and the sensitive lines should suffer from similar errors (as these are independent of the field). The existence of a trend in the magnetic diagnostic plot can only be due to a magnetic field, so long as the sensitive lines have the same response, on average, to errors in the model as the insensitive lines. This can be checked by plotting magnetic sensitivity against those line parameters which would respond to errors in abundance or temperature. In Figure 3 we show that the magnetic sensitivity in our lines is not a function of either W_{eq} or excitation potential. Furthermore the line excitation potentials are all between 2 and 5 eV, so they are not extremely sensitive to temperature changes in G and K stars. This makes it unlikely that a slope seen in the magnetic diag-

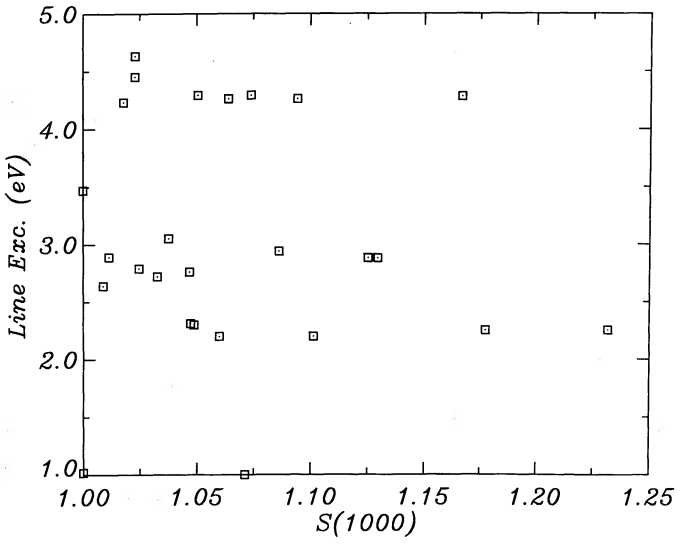

FIG. 3a

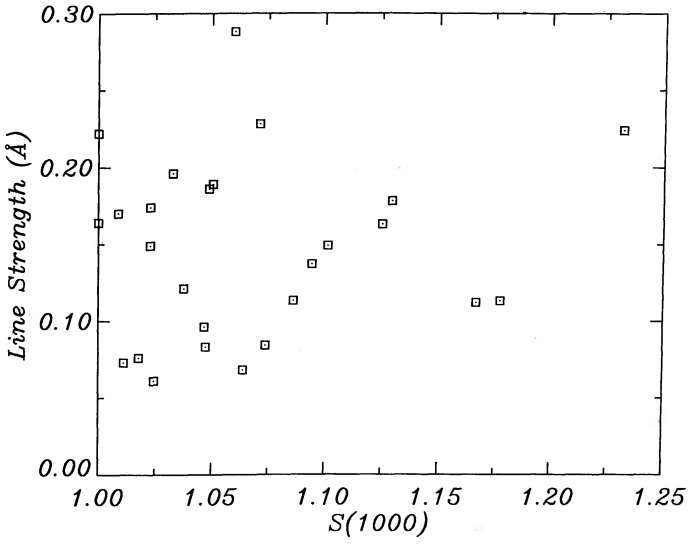

FIG. 3b

FIG. 3.—(*a–b*) Two demonstrations that our line samples should not be sensitive to atmospheric parameters in the magnetic diagnostic diagrams. Panel *a* shows that the excitation potential of the lower levels of the lines is uncorrelated with magnetic sensitivity (the factor S_{1000} is explained in the text). Panel *b* shows that the line strength (observed equivalent widths in TAP 35) is also uncorrelated with magnetic sensitivity.

nostic plot is a result of some systematic problem in the model atmosphere. Just to be sure, we later check the results by computing the magnetic diagnostic with different atmospheres.

It also means that we are relatively insensitive to the fact that the real stellar atmosphere contains a number of different thermal structures, inside and outside magnetic regions. Even if lines are systematically stronger or weaker in magnetic regions due to thermal differences, the effects will occur in the magnetically sensitive and insensitive lines equally. Such thermal mixing will therefore increase the scatter in our diagnostic plot (and may indeed be a major contributor to the scatter we see). It will, however, not introduce spurious magnetic detections, and primarily has the effect of rendering upper limits on nondetections less strict than they otherwise would be.

4.2. *Main-Sequence Stars*

The most obvious way to test our proposed new method is by trying it on the Sun. The Sun as a star is very inactive, and we would have no hope of seeing its fields with this method (even profile methods fail). Since spatial resolution is possible, however, one can test the method on solar magnetic regions. These are either bright (plage) or dark (sunspots). In the stellar case the magnetic signal will tend to be dominated by the bright regions, unless the dark regions dominate in area. Unfortunately, even solar plage is not that active compared to the active stars we are interested in. The filling factor in plage tends to be 10%–20%, with field strengths $\sim$1500 G. This means $Bf \lesssim 300$, which is less than even active main-sequence stars. On the other hand, the quality of solar data is very high, and its atmosphere is relatively well understood.

At the suggestion of the referee, we performed the clearest and easiest solar test we found. Brandt & Solanki (1990) reported the equivalent widths of a set of lines, measured both in and out of a plage. It is well known that the neutral metal lines tend to weaken in plage, presumably because the atmosphere is hotter there. This weakening runs counter to the Zeeman enhancement we are looking for. But since the effect occurs equally for sensitive and insensitive lines, it would be calibrated out by us as a metallicity reduction. The real question is whether the lines exhibit a systematic enhancement in their equivalent widths with increasing magnetic sensitivity. Using the full set of their lines, a plot of W_{eq}(plage)/W_{eq}(quiet Sun) versus Landé g shows no clear trend. Included among the lines, however, are a few which are very sensitive to temperature because their excitation potentials are less than 1.1 eV. Given that the plage observed only has a filling factor of 12%, the line weakening is relatively severe for such lines and easily overwhelms any Zeeman enhancement. Since we do not use such temperature-sensitive lines in our method, we eliminated them from the list of Brandt & Solanki and produced Figure 4, which shows W_{eq}(plage)/W_{eq}(quiet Sun) versus Landé g. Despite the use of Landé g as abscissa instead of true magnetic sensitivity, S_{1000}, the Zeeman enhancement in the plage is clearly evident. The small amount of the enhancement is consistent with the relatively low magnetic flux that should be there. Note that the ordinate is not quite analogous to what we use in our stellar analyses in that the numerator and denominator represent differences in thermal structures. Nonetheless, the Zeeman enhancement of line equivalent widths is apparent.

We also tried to perform our analysis directly on resolved solar observations we made with the Hamilton. In those cases we could not control how much contamination by quiet, plage, and sunspot regions were in each spectrum. A spot was clearly in our spot spectrum, and both it and our plage spectrum had a strong reversal in the Ca II IR triplet (stronger than in TAP 35). We do not present plots of the results because we do not really know what they should look like, given the unknown contamination effects. Suffice it to say that the plage plot looks a lot like our TAP 10 result, and the spot plot looks a lot like our TAP 35 result (both discussed below). This test therefore is consistent with the proposition that the method works, but does not add extra conviction. We also tried the method on an FTS umbral spectrum (kindly provided through NSO by M. Giampapa). The main thing we learned from it is that a different set of diagnostic lines is required to do very cool atmospheres well, because of the behavior of the magnetic curve of growth discussed in the last section. A more detailed discussion of this will appear in a subsequent paper in which we study late K and M stars. What can be said is that the observed results were again consistent with the effect we calculate.

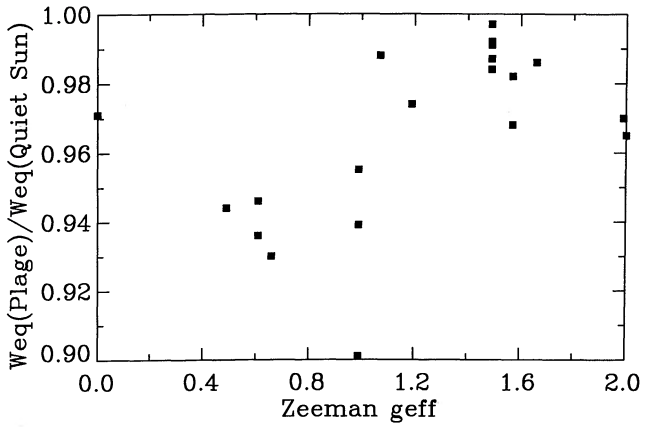

FIG. 4.—The enhancement of equivalent widths of Zeeman-sensitive lines in solar plage compared to quiet solar regions. The ratio of equivalent widths in plage relative to quiet Sun shows a correlation with Zeeman g_{eff}. This suggests that measurements of equivalent widths in stellar spectra permit detection of magnetic fields. (Data taken from Brandt & Solanki 1990.)

We then checked to see if ξ Boo A had a field detectable by this method. Its diagnostic plot is given in Figure 5*a*. Two things are clear: the level of scatter is fairly small compared with the effects of say, a 1500 G field covering the whole star, and there is little evidence of a positive slope, i.e., no convincing field detection. Indeed, the scatter is barely larger than the measurement error which is a testament to the similarity between ξ Boo A and the star which was used to calibrate the line strengths: 61 UMa. Since the latter is relatively inactive, this calibration should not have substantially reduced the sensitivity of this method to magnetic fields by masking them in the determined atomic strength of the sensitive lines. We can estimate the lower detection limit by finding what flux would yield a 1 σ deviation from zero at the right edge of the plot. This corresponds to $Bf \lesssim 500$ G, which is compatible with our determination for this star in Marcy & Basri (1989). The reason for our lower sensitivity here is that we are relying only on equivalent width changes, instead of using the information in the line shape itself as before. The loss of sensitivity is of course compensated by the ability to study more rapidly rotating and fainter stars.

The results for ϵ Eri are shown in Figure 5*b*, and are qualitatively similar. The scatter is nearly twice as large than for

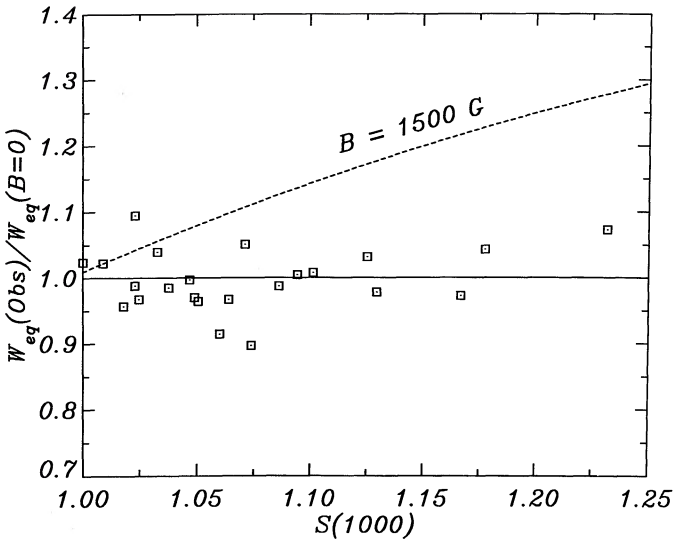

FIG. 5a

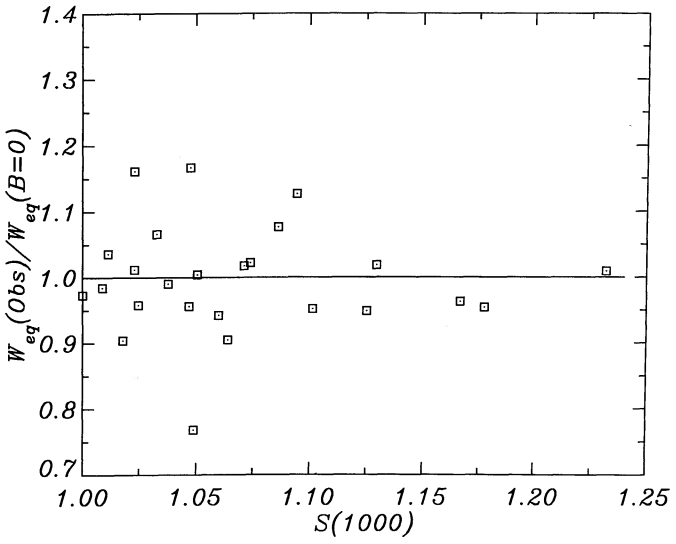

FIG. 5b

FIG. 5.—(*a–b*) Magnetic diagnostic plots for two main-sequence stars. The abscissa is the ratio of computed line equivalent width at 1000 G to 0 G, while the ordinate is the ratio of observed equivalent widths to the computed value at 0 G. The computations use oscillator strengths derived to yield perfect agreement with observations of 61 UMa. The Panel *a* shows the very good agreement in the magnetic G8V star ξ Boo A, and also that this method is not capable of detecting a magnetic field in an active main-sequence star. Panel *b* shows the somewhat greater scatter in the active K2V star ϵ Eri. Here too, no field is detected.

ξ Boo A, probably because of the cooler atmosphere compared to the calibration star (see § 3.1). Again, however, there is no real evidence of a magnetic field with a sensitivity limit somewhat worse than for ξ Boo A (< 750 G). Again, this is compatible with the measured field on this star from Marcy & Basri (1989). It appears from these cases that if we are to be able to detect magnetic fields on pre–main-sequence stars, they would have to be substantially larger than those on active main-sequence stars. Fortunately, such a proposition is reasonable in light of the larger X-ray and emission line fluxes seen in very young stars.

4.3. *TAP 35*

The magnetic diagnostic plot for TAP 35 is shown in Figure 6. It is obvious that the scatter is substantially worse than for ξ Boo A. This is presumably due to some errors in the model atmosphere, since the measurement errors are substantially less than this scatter, and the adopted line strengths were successful in the case of ξ Boo A. There are no ratios below unity when S_{1000} is larger than 1.08, which is about at the value where the magnetic field should produce an effect larger than the measurement error. We quote errors on our magnetic measurement based on the overall scatter, to be conservative. The 1 σ error in a quadratic fit to the ratio points is 0.10. The scatter is less for the sensitive lines ($S_{1000} \geq 1.08$), although we can think of no reason why this should be so. The 1 σ error about the 1000 G predicted values for these lines is 0.07. With such large scatter it is difficult to make an accurate determination of the magnetic field, but the presence of the field seems fairly firm. What is even firmer is that the effects of a 2000 G field over the entire star are not seen in the data.

We explored the nearby parameter space to find the model which produced the least scatter in the magnetic diagnostic plot. The basic result was rather insensitive to changes in temperature within 500 K, or changes in abundance within 0.5 dex. The best model that we tried had $T_{\rm eff}$ of 4900 K and log (Fe/H) = −4.4. Results from it are shown in Figure 6, which is only a slight improvement over the original model. Here the 1 σ error to the fit is reduced only slightly, but the sensitive lines are generally less scattered. It would clearly be desirable to have better spectral typing, so the basic model parameters were less uncertain. This probably will not change the basic results of the magnetic analysis, however. The primary result is that, even given the large scatter in Figure 6, an upper limit of $Bf \lesssim 1500$ G is implied by the fact that the

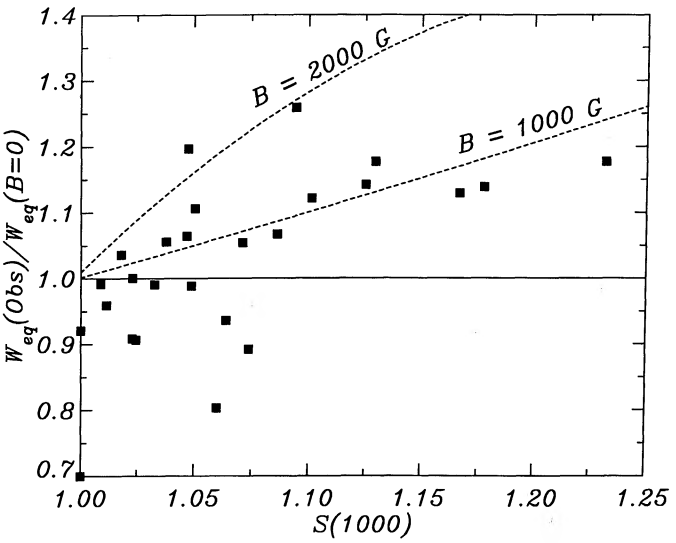

FIG. 6.—Magnetic diagnostic plot for TAP 35. The abscissa is the ratio of computed line equivalent width at 1000 G to 0 G, while the ordinate is the ratio of observed equivalent widths to the computed value at 0 G. The dashed lines are fits to the predicted loci of points for 1 and 2 kG fields. The predictions assume unit filling factor, but are roughly valid for any product of field strength and filling factor giving the quoted values. A product (ignoring polarity) Bf of ~ 1000 G is apparently measured on TAP 35.

points in the right of the plot all lie well below their predicted positions if the star had been covered by 2000 G fields (upper dashed curve). This result seems rather firm; we can think of nothing that would push the points that high, and the net effect of all errors in the analysis is already apparent in the scatter of the insensitive lines.

Our philosophy here, since we are developing a new technique, is that if any combination of parameters can be found which eliminates the magnetic detection then no firm detection can be claimed. We therefore carried out a number of tests in which we tried to eliminate the positive slope in Figure 6 by changing models. As mentioned above, making mild changes in the abundance or temperature did not significantly affect the result. We also checked to see if a substantially lower gravity could play a role (since the stellar gravity is poorly determined). This was done at log (g) = 3.5, with temperatures of 5250 and 4900 K. Of course, we had to adjust the abundances to reflect the change in gravity; a new abundance was derived in each case with the same procedure as the original determinations. In both cases, the resulting magnetic diagnostic plot had scatter similar as before and showed a slightly stronger field (with the λ8468 ratio above 1.3). This means that our quoted field strength is actually an underestimate if we have overestimated the gravity.

Finally, we checked a model with heating in the upper photosphere, as might be expected in a star with a strong chromosphere. This model is a scaled HM model with temperature held constant at its value at $\tau_{5000} = 10^{-3}$ above that point. This has the effect of filling in the cores of the stronger lines, and thereby makes the ratio of observed to null W_{eq} increase because of a decrease in its denominator. We found that this had essentially no effect on the magnetic diagnostic, because the lines respond to heating in a way that is independent of the magnetic field since line strength is independent of S_{1000}. Since λ8468 had one of the larger amounts of core filling, the field measurement was increased, if anything. There is undoubtedly some filling in actually present in the observations, since the very strong lines like Hα and the Ca II IR triplet are filled to the point of emission. In summary, we were unable to eliminate the basic detection of the magnetic field by any of the changes in model that we tried, and several of them actually yielded stronger detections. On that basis we claim detection of magnetic field on TAP 35, with a "flux" value of $Bf = 1000 \pm 500$ G. A simple correlation analysis on Figure 6 yields a greater than 99.9% confidence that the axis variables are correlated. Of course, this result has a lower certainty than the upper limit, given the large scatter in the trend.

Finally, if all this modeling remains unconvincing to the reader, we present a purely observational test with the indication that there are somewhat (but not excessively) stronger magnetic fields on pre–main-sequence stars than on active main sequence stars. In Figure 7 is shown the magnetic diagnostic plot, except instead of using theory as part of the ratio in the ordinate, we simply use the ratio of equivalent widths in TAP 35 to those in 61 UMa (which is moderately active for a main-sequence star). The result is in the same direction as that of Figure 6. The scatter in the insensitive lines reflects the fact that these two stars are only somewhat similar. The normalization of the ratio has been changed to compensate for the difference in metallicities, by making the median of the insensitive lines unity. The four most magnetically sensitive lines fall above the unit ratio, while only half the insensitive lines do. This means that the magnetically sensitive lines are preferentially stronger than the insensitive lines on TAP 35 compared to 61 UMa, independently of atomic or stellar parameters. Again, there is no reason that a trend with magnetic sensitivity should be seen unless there really is Zeeman enhancement of the lines. Of course, such an observational plot cannot tell us what the field strength is (and theory was still needed to produce the abscissa). Further, this simple diagnostic shows again that the fields on TAP 35 are not many times greater than on 61 UMa, since the trend in Figure 7 is so weak.

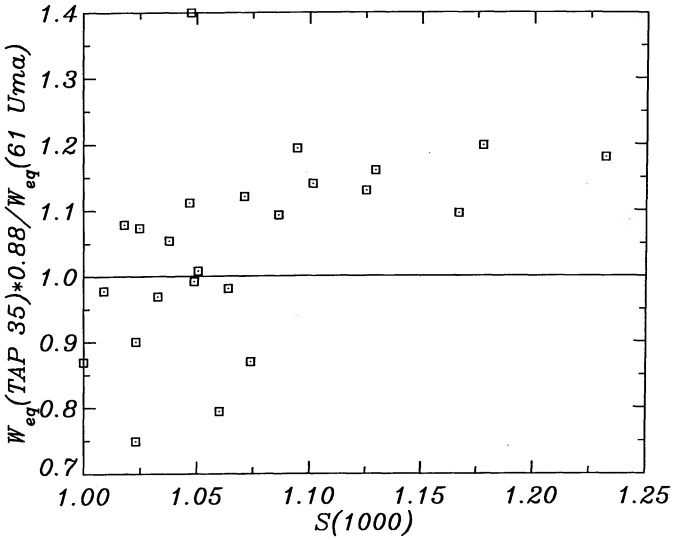

FIG. 7.—An observational "magnetic diagnostic." Here the ordinate ratio is simply between the observations of TAP 35 and 61 UMa, where 61 UMa has replaced the computed null field line strengths of the previous two figures. There is still a correlation of the line ratios with magnetic sensitivity, implying that there is a measurably greater field on TAP 35. The ordinate ratio has been adjusted to make the median of the insensitive line ratios near unity.

4.4. *Limits on the Maximum Field Strength*

Because in the preceding analysis we have used the equivalent widths of lines to detect Zeeman broadening, rather than the line profiles, the results really only give a measure of Bf. Previous work and tests we made here show that there is a fairly even trade-off between the field strength and filling factor, at least within changes in the field strength of less than a factor of 2. On the other hand, we showed in § 3.3 that the growth in equivalent width with magnetic field strength depends on the characteristics of the transition, and that some lines grow strongly at higher field strengths while others have "saturated" on the magnetic curve of growth. In the analysis here, we assume that the atmosphere is the same inside and outside of magnetic field regions. Basri, Marcy, & Valenti (1990) showed that this is not necessarily safe, but given the crude and pioneering nature of this work it does not make sense to worry about that yet. There is therefore a simple expression for the filling factor that will produce the observed equivalent width of a line at a specified calculated field strength, given calculated values for the null profile:

$$f(B) = \frac{W_{eq}(\text{obs}) - W_{eq}(0)}{W_{eq}(B) - W_{eq}(0)} .$$

TABLE 3

LIMITS ON FILLING FACTORS[a]

B (G)	$\langle f \rangle$[a] (%)	σ_f (%)	f_{max} (%)	$B\langle f \rangle$ (G)	$B\sqrt{\langle f \rangle}$ (G)
2000.....	50	19	69	1010	1420
3000.....	34	12	46	1020	1750
4000.....	29	12	41	1160	2150
5000.....	26	13	39	1300	2550

[a] Based on the six most sensitive lines.

The best line to place limits on high field strengths is λ7491, as can be seen from Figure 2. If both our measurements and our models had no error, the above formula tells us that there cannot be more than a 10% covering factor of fields 3000 G or larger. Of course, we know there are errors, so a more conservative approach is to use the six most sensitive lines, and simply average their limits. The limits found in this manner are listed in Table 3. They are unfortunately not particularly stringent. The only statement we can make with confidence is that not more than half the star is covered by fields 3000 G or larger; and quite probably this limit can be reduced to a third of the star. There is more we can do to place limits, however.

The other approach to finding limits on the higher field strengths that might be present is to turn again to profile information. While the profiles observed display only rotational broadening, they would in fact show Zeeman broadening if the fields were sufficiently strong. The line most likely to show this is λ8468, which has the highest Landé g at the longest wavelength in our sample. For this line, the null field case (after rotational broadening) has a core which is significantly shallower than the observed profile. At field strengths above 3500 G, the separation of the σ components becomes large enough that again the core of the calculated line becomes shallower than observed. This means that for *any* filling factor for $B > 3500$ G the computed profile is too shallow. Furthermore, above 4000 G the Zeeman broadening is sufficient to show up even at a rotational velocity of 17 km s^{-1}. We can therefore rule out any significant (more than 10% covering factor) occurrence of fields 4000 G or stronger on TAP 35, subject of course to possible errors in our observations or models. The same analysis for 3000 G fields yields cores too deep for $f > 40\%$ and cores too shallow for $f < 20\%$. At 2000 G, the core is too deep if the star is more than half covered by such fields. The results for other lines make the allowed regions for these moderately strong fields rather unlikely, however. Thus we conclude from a profile analysis that a significant concentration of fields 3000 G or stronger is unlikely.

The conclusion of this section is that although the equivalent width analysis by itself does not specify the field strength and filling factors separately, the field we have detected is unlikely to be as strong as 3000 G. Combinations of B and f which yield a product of 1000 G and have fields less than 3000 G are probably equally plausible for TAP 35 based on our analysis. We should note that the optical lines we are using are insensitive to fields which may be present in dark starspots. These fields could be strong, but due to the low contribution of the spots to the integrated flux from the star, the observed line strengths would not be significantly affected. The presence of spots could, in principle, be inferred from low-excitation lines, or from the light curve. Lines in the infrared would be more useful in diagnosing spot fields.

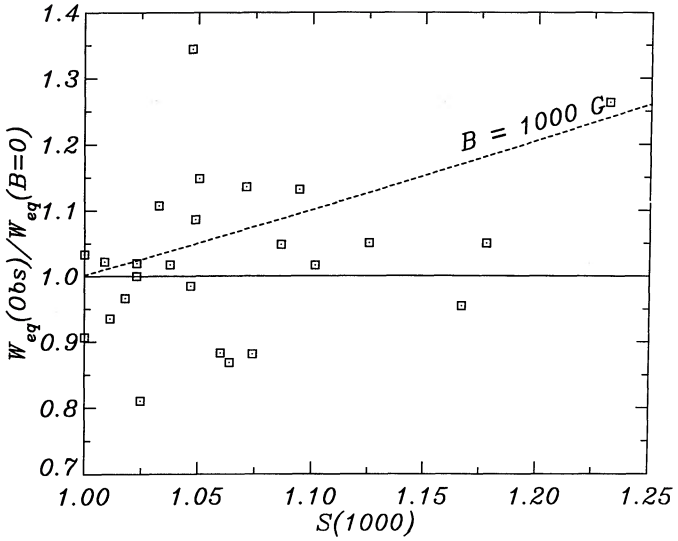

FIG. 8.—The magnetic diagnostic plot for TAP 10. In this case there is no real evidence of a detected field on this hotter and less active young star. Tests with other choices of atmospheric parameters did not change this result.

4.5. *TAP 10*

The analysis of the star TAP 10 proceeds very much as with TAP 35. We settle on a best guess of 5250 K and log (Fe/H) = −4.48. The temperature is a little cooler than expected from the spectral type, but gives the least correlation between the line excitation of our insensitive lines and their ratio of observed to calculated equivalent width. We check our results with both hotter and cooler temperatures to insure that our result is not dependent on this choice of temperature. The magnetic diagnostic plot is shown in Figure 8. In this case, we do not detect a perceptible field. Although λ8468 is consistent with a 1000 G field, the other sensitive lines do not bear this out (and of course there are insensitive lines similarly scattered upward). This means that the field on TAP 10 is below our detection threshold: $Bf \lesssim 700$ G. The need for many lines is illustrated by this case; we do not understand why λ8468 is higher than the other sensitive lines. A result based primarily on it would obviously differ from the multiline answer. Because of all the potential problems in this sort of analysis, it is important to have enough lines formed in different ways to lend statistical credence to a result.

We looked into the individual observations of λ8468 to make sure its anomalous position was not due to a problem in one of the observations. We also made the diagnostic plot for 5500 K and 4900 K, adjusting the Fe/H in each case. The results were quite similar, and 5250 K was the one with the least scatter. We must therefore conclude that the total magnetic flux on TAP 10 really is less than on TAP 35. This result is not entirely surprising, since the results for the main-sequence stars (Saar 1990) show that the hotter stars (with shallower convection zones) tend to have less magnetic flux, and TAP 10 is also a slower rotator than TAP 35 (except for the unknown inclination angles).

There is a check on whether this result is reasonable, since the implication would be that the chromospheric activity should be less on TAP 10 than TAP 35. It is clear in Figure 1 that the emission core of the Ca II infrared triplet line at λ8498 is stronger on TAP 35, but one must compensate for the photo-

spheric contrast which will be larger on the cooler star. We therefore divided each star by a spectroscopic standard with the same spectral types (K1 and G5). The *residual* emission feature after correction for rotation and division should be a better indicator of the relative intrinsic chromospheric strengths. There were no gross problems with the procedure as the metallicities were fairly similar, since photospheric lines (like λ8468 !) divided out nicely (Fig. 1). Remember that the magnetic enhancement is only a few hundreths of angstroms in equivalent width. The equivalent widths of the resulting pseudo-emission features for the triplet line in TAP 10 and TAP 35 were -0.26 Å and -1.10 Å, respectively. This large a difference confirms that TAP 10 has a weaker chromosphere in concert with its weaker magnetic field. Any problems with how closely this procedure really measures intrinsic activity levels are likely to be much more subtle. Obviously, it will be important to check a number of other cases before making any generalizations.

In summary, we have probably detected a magnetic field on TAP 35. The total magnetic flux is about a factor of 2 larger than is found on very active main-sequence stars. We can say with confidence that the fields on these WTTS are not 5 or 10 times stronger than on active main-sequence stars. We did not find a field on TAP 10, but are not greatly surprised by this because the star is apparently less active. Our method has been shown to be useful for placing limits to the magnetic flux on stars that are much fainter and/or more rapidly rotating than could be analysed by previous methods employing line profiles. It should allow a study of fields on T Tauri stars, RS CVn stars, and dMe stars; all of which were very difficult or impossible to study before. The method can clearly benefit from a refined analysis of the atmospheric structure of these stars and from adding more lines, especially in the near infrared. Different lines should be chosen when moving to different spectral types.

We would like to acknowledge the support of the National Science Foundation for this work, through grants AST-8911596 to G. B and AST-8919634 to G. M. The data used in this work were obtained at the Lick Observatory, which is operated by the University of California and partially supported through a block grant from the NSF. We thank the referee for helping strengthen our presentation, and M. Giampapa for supplying a solar umbral spectrum.

REFERENCES

Arribas, S., & Crivellari, L. 1989, A&A, 210, 211
Basri, G. 1991, Mem. Soc. Astron. Ital., 61, 3, ed. R. Pallavicini, 707
Basri, G., & Batalha, C. 1990, ApJ, 363, 654
Basri, G., & Marcy, G. W. 1988, ApJ, 330, 274
Basri, G., Marcy, G. W., & Valenti, J. A. 1990, ApJ, 360, 650
Bertout, C., Basri, G., & Bouvier, J. 1988, ApJ, 330, 350
Blackwell, D. E., Petford, A. D., & Simmons, G. J. 1982, MNRAS, 210, 595
Brown, D., & Landstreet, J. 1981, ApJ, 246, 899
Bouvier, J. 1990, AJ, 99, 946
Brandt, P. N., & Solanki, S. K. 1990, A&A, 231, 221
Calvet, N., Basri, G., & Kuhi, L. V. 1984, ApJ, 277, 725
Cohen, M., & Bieging, J. H. 1986, AJ, 92, 1396
Cram, L. 1979, ApJ, 234, 949
Feigelson, E. D. 1987, in Cool Stars, Stellar Systems, and the Sun, ed. J. L. Linsky & R. E. Stencel (Berlin: Springer), 455
Finkenzeller, U., & Basri, G. 1987, ApJ, 318, 823
Fuhr, J. R., Martin, G. A., & Wiese, W. L. 1988, J. Phys. Chem. Ref. Data, 17, No. 4
Gray, D. F. 1976, The Observation and Analysis of Stellar Photospheres (New York: Wiley)
Hartmann, L., Calvet, N., Avrett, E. H., & Loeser, R. 1990, ApJ, 349, 168
Hartmann, L., Hewitt, R., Stahler, S., & Mathieu, R. D. 1986, ApJ, 309, 275
Hartmann, L., & Kenyon, S. J. 1990, ApJ, 349, 190
Herbig, G. H. 1970, Mem. Roy. Soc. Sci. Liége, 19, 13
Holweger, H., & Müller, E. A. 1974, Solar Phys., 39, 19
Imhoff, C., & Giampapa, M. 1982, in Advances in Ultraviolet Astronomy: Four Years of IUE Research, ed. Y. Kondo, J. M. Mead, & R. D. Chapman (NASA SP-2338), 456
Jefferies, J., Lites, B. W., & Skumanich, A. 1989, ApJ, 343, 920
Johnstone, R. M., & Penston, M. V. 1986, MNRAS, 219, 927
———. 1987, MNRAS, 227, 797
Königl, A. 1989, ApJ, 342, 208
———. 1991, ApJ, 370, L39
Kurucz, R. L., Furelid, I., Brault, J., & Testerman, L. 1984, Solar Flux Atlas from 269 to 1300 nm, National Solar Observatory Atlas, No. 1
Lago, M. T. V. T. 1984, MNRAS, 210, 323
Marcy, G. W., & Basri, G., 1989, ApJ, 345, 480
Montmerle, T., Koch-Miramond, L., Falgarone, E., & Grindlay, J. E. 1983, ApJ, 269, 182
Rutten, R. J., & Kostik, R. I. 1982, A&A, 115, 104
Saar, S. H. 1990, IAU Symp. 138, Solar Photosphere. Structure, Convection, and Magnetic Fields, ed. J. O. Stenflo (Dordrecht: Kluwer), 427
Solanki, S. K., & Stenflo, J. O. 1985, A&A, 148, 123
Shu, F. H., Lizano, S., Ruden, S. P., & Najita, J. 1988, ApJ, 329, L19
Vrba, F. J., Rydgren, A. E., Chugainov, P. F., Shakovskaya, N. I., & Weaver, W. B. 1989, AJ, 97, 483
Walter, F. M. 1987, PASP, 99, 31
Walter, F. M., Mathieu, R. D., Myers, P. C., & Vrba, F. J. 1988, AJ, 96, 297